Journal of
Composites Science

MDPI

Article

Magnetic Resonance Imaging as a Tool for Studying Soy-Based Adhesives in Plywood

Joseph J. Marcinko [1,*], Anthony A. Parker [2], James H. P. Collins [3] and Josh Tyler [4]

[1] Polymer Synergies LLC, 5316 Lena Road, Suite 102, Bradenton, FL 34211, USA
[2] A.A. Parker Consulting LLC, 11161 E State Rd 70, Suite 110–570, Lakewood Ranch, FL 34202, USA
[3] Advanced Magnetic Resonance Imaging and Spectroscopy (AMRIS) Facility, National High Magnetic Field Laboratory (NHMFL), University of Florida, Gainesville, FL 32610, USA
[4] Columbia Forest Products, 242 Columbia Forest Products Road, Craigsville, WV 26651, USA
* Correspondence: drjoe@polymersynergies.com

Abstract

Magnetic resonance imaging (MRI) is a well-established technique used in medical applications and bio-based research. It has also been used to study wood and composite materials of various types. Soy-based adhesives used in hardwood plywood applications are not very moisture-resistant. We have employed MRI to study water-soaked plywood composites made with soy adhesives in an attempt to gain insight into how water interacts and affects the soy adhesive bondlines. Various MRI data acquisition sequences were used to show how water interacts and migrates within the soy adhesives and to quantify the presence of water at the bondline of the plywood samples. The data from MRI was combined with cyclic testing data of plywood to help understand how soy adhesives can be modified to reduce their moisture sensitivity. MRI of plywood bondlines made with chemically modified soy adhesives shows that moisture ingress can be reduced dramatically. Cyclic water soak/drying testing of plywood made with chemically modified soy adhesives shows that the reduction in moisture sensitivity results in dramatic improvements in bondline durability, as measured by the ANSI/HPVA EF 2020 cyclic testing protocol for hardwood plywood.

Keywords: soy adhesives; magnetic resonance imaging; moisture resistance; plywood

1. Introduction

Magnetic resonance imaging (MRI) is a nuclear magnetic resonance (NMR) characterization technique that relies mostly on the detection of water either within the human body or within a material. More specifically, each hydrogen atom in water has a nucleus that consists of a single proton. These protons are very sensitive to the resonance effects of external magnetic fields that the atomic nuclei of water experience in these magnetic fields [1–3]. The protons within the water molecules behave like tiny magnets. When placed in a strong magnetic field, these protons align with the direction of the field. The MRI instrument uses radiofrequency pulses that knock the aligned proton nuclei out of their equilibrium position with the magnetic field. When the radiofrequency pulse is turned off, the protons return to their original alignment. As they do so, they emit faint radio signals. Electronic receiver coils in the MRI instrument detect these emitted signals. The data is processed to construct detailed images of the water within the material (or person) based on the signal from the protons within the water. The contrast in MRI images depends on how quickly the hydrogen nuclei from water return to equilibrium and emit signals. MRI

Check for updates

Academic Editor: Konstantinos Tserpes

Received: 17 August 2026
Revised: 15 September 2026
Accepted: 16 September 2026
Published: 21 September 2026

Copyright: © 2026 by the authors. Licensee MDPI, Basel, Switzerland. This article is an open access article distributed under the terms and conditions of the Creative Commons Attribution (CC BY) license.

scans can be tailored to highlight specific types of water, either bound or restricted-mobility water or mobile water, by adjusting the timing and strength of the radiofrequency pulses. The spin–lattice relaxation time (T_1) and the spin–spin relaxation time (T_2) are commonly used to create diffusion-weighted images, each providing unique information about the water within the material (or person). Free or mobile water molecules rapidly tumble and are inefficient at transferring energy to the surrounding lattice. This means they take a long time to realign their magnetization with the main magnetic field, resulting in a long T_1 value. Water molecules that are bound (hydrogen-bonded) to larger macromolecules, such as proteins or wood, take on the slower motion characteristics of these macromolecules. This slower motion of bound water makes it more efficient at relaxing, meaning it transfers energy to the lattice more effectively and recovers its longitudinal magnetization more quickly, leading to a shorter T_1 time. Thus, the bound water appears brighter on the images. Likewise, bound water will have short T_2 relaxation times compared to mobile water. Because of the restricted motion of the bound water, rapid spin–spin dephasing of the MRI signal occurs, and bound water appears darker in T_2-weighted images. These differences in contrast are used to define the state of water within a structure (or a person) and give rise to the images we observe.

In material science, MRI has been employed to non-destructively investigate the internal structure and composition of various materials. One of the first examples of this was obtaining cross-sectional images of three poly(vinyl alcohol) (PVOH)-stabilized poly(vinyl acetate) (PVAc) emulsions in glue lines between a wood block and a ceramic tile [4]. There have also been numerous papers and reviews related to the use of MRI to study the moisture in wood [5–8]. One specific example used MRI to study diseased wood. MRI revealed pathological anatomical features of coast live oak trees (*Quercus agrifolia*) that were naturally infected with *Phytophthora ramorum*. In this study, infected areas were compared to healthy sections of the wood. Various infected tissues were revealed, and the depth of infection into the xylem could be estimated by T_1 and T_2 images [9]. A more recent illustration of MRI used in wood composites was to study mass timber. This work established that MRI can be useful to support mass timber moisture durability studies. MRI allowed identification of features such as joints, growth rings, and layers in pine/spruce cross-laminated timber (CLT) samples at a resolution of slightly less than 1 mm [10].

Within this paper, we describe how we used MRI to study the association of water with soy adhesive bondlines in plywood. Soy adhesives are of great interest to wood composite manufacturers as a sustainable alternative to conventional petroleum-based adhesives. However, since the patenting of these adhesives for use in wood composites in 2007, the technology has changed very little, and market growth has been minimal because of the poor moisture resistance of soy-based adhesives. To overcome the moisture-resistance problem, it would be helpful to understand more about the mechanism of how water affects the compositional chemistry of soy adhesives and how this chemistry in turn influences adhesion at the bondline. With a better understanding of the reasons for moisture-induced adhesive failures, it should become possible to test and develop chemistry-specific solutions to overcome the moisture-resistance problem.

We have previously reported on the chemical changes occurring within the soy adhesive bondlines of wood composites when they are exposed to moisture [11,12]. That work described the chemistry of the water-soluble components within the bulk adhesive and the migration of these components into the wood and at the wood–adhesive interface. The presence of these water-soluble components at the interface results in a weak boundary layer which is susceptible to moisture. The data presented herein will describe how water migrates and associates with the soy adhesive at the plywood interface.

2. Materials and Methods

Soy adhesives were prepared, as previously described, from a dispersion of 200/70 (mesh/PDI) soy flour in water at a 38 percent total solids concentration [11,12]. A 200 mesh is the particle size of the soy particles, which equates to an average particle size of 74 microns, and PDI is the Protein Dispersity Index for the soy flour, which relates to how well the soy flour disperses in water. One of the adhesive samples was prepared using a 30 percent solids polyamideamine-epichlorohydrin (PAE) resin as a crosslinker for the adhesive. The concentration of the PAE solids in the adhesive was 4 percent; thus, the final 38 percent solids adhesive consisted of 96/4 w/w soy-flour components and PAE components. This sample was labeled 67-3. A second adhesive was prepared having a 38 percent soy solids composition without PAE; thus, it consisted of 100 percent soy flour solids and was labeled 67-4.

Another soy adhesive dispersion was prepared using magnesium oxide (MgO) as an ionic crosslinker. MgO has been shown to be an alternative to PAE as a crosslinker for soy adhesives [13]. This adhesive was also composed of 200/70 soy flour, and the ratio of MgO to soy was 5/1. The total adhesive solids concentration for this adhesive was also 38 percent.

Surface-treated soy meal (STSM) was prepared using a proprietary hydrophobic chemistry, which was dry-blended onto ground soy meal of a 325 mesh (45 micron) particle size. The surface-treated soy meal was post-treated at 80 °C for 2 h. The surface-treated soy meal was substituted into some of the Soy/MgO adhesives, replacing one percent or two percent of the 200/70 soy flour with STSM. The objective of surface treating the soy meal is to render it hydrophobic and use it as an additive for soy adhesives to assist in moisture resistance and bondline durability.

Three-layer plywood samples were prepared using 0.125-inch-thick yellow poplar (*Liriodendron tulipifera*). The plywood specimens were prepared using Soy/PAE or Soy/MgO adhesives. Thirty grams of the wet soy-based dispersions were applied to the loose face of a 30.48 cm × 30.48 cm (12″ × 12″) poplar veneer. A second poplar veneer was then placed on top of the adhesive, loose face to loose face, with the grain direction perpendicular to the bottom veneer layer. Another 30 g of adhesive was applied to the top surface of the second veneer, and a third veneer, loose-face down, was placed on top of the adhesive layer with the grain perpendicular to the second veneer layer. The multilayered assemblies were then pressed at 130 °C for 4 min while under a pressure of 1.03 MPa (153 PSI).

Some of the Soy/MgO plywood samples were sent to an external laboratory for ANSI/HPVA EF 2020 cyclic testing [14]. The testing procedure subjects hardwood plywood samples to rigorous, repeated wetting and drying to accelerate bondline stress. The residual wood from the cutting of the EF 2020 samples was sent back to the Polymer Synergies lab for imaging studies.

Samples for imaging studies were cut from the 3-layer plywood sample residuals from the ANSI/HPVA EF 2020 cyclic testing. The imaging samples were 10 mm × 10 mm cubes or 10 mm-diameter cored cylinders.

The MRI studies were conducted at the University of Florida's National Magnet Laboratory in Gainesville, Florida, using a Bruker 750 MHz (17.6 Tesla) Solution/Solid State NMR & Preclinical MRI equipped with a Bruker NEO console. MR images were acquired with Paravision 360 3.5. The plywood samples were soaked for 24 h prior to imaging. The samples were then removed from water, placed in a stoppered test tube, and placed in the imaging coil in the magnet. Several MRI pulse sequences were tested to determine the best methods for imaging the water-soaked plywood samples. Due to the short T_2 relaxation time of the water contained within the samples, a ZTE (zero echo time) sequence [15,16] was used. This sequence allows for the water content of the wood and

adhesive to be measured in a single 3D image. The images were acquired with a resolution of 128 × 128 × 128 voxels, over a 20 mm cubic volume, leading to an isotropic voxel size of 0.156 mm. A repetition time of 0.76 ms and a flip angle of 4° were used. With 32 averages per scan, the total scan time was 21 min. The acquisition bandwidth was optimized to minimize artifacts caused by the rapid ZTE sequence. Image slices were extracted in post-processing from the center of the samples to analyze water distribution within them and its changes over time, as well as to visualize the adhesive/wood interfaces. 3D images and movies were produced using Paravision software to further visualize the wood and adhesive layers. ZTE images had no significant T_2 signal contrast due to the effectively zero echo time used in the sequence. T_1 contrast can arise due to the short repetition time. The signal was T_1-weighted, meaning that longer T_1 times led to decreasing MR signal. T_1 estimates were made using a sequence of 2D spin-echo images (echo time 2.5 ms, recycle delays varied from 150 ms to 2000 ms, resolution of 128 × 128 voxels of 20 mm × 20 mm, with a slice thickness of 0.5 mm) acquired on a sample soaked for 24 h. T_1 values of between 900 and 1200 ms were measured in saturated regions of the wood, and of between 600 and 900 in the saturated bond layers. This corresponded to a 30–60% increase in relative signal in the bond layer compared to the other regions of the wood due to T_1 contrast effects. It should be noted that T_1 could not be accurately measured using standard methods in less saturated samples due to the short T_2 relaxation times. Additional MR images using FLASH, a low-flip-angle gradient echo technique, were also acquired [17]. An echo time of 0.6 ms, repetition time of 70 ms, and excitation angle of 20° were used. An in-plane resolution of 0.156 mm was used with a slice thickness of 2.5 mm. Eight scans were used, with a total acquisition time of 1 min. These were primarily used to confirm positioning of the sample, as they could only detect residual surface water or heavily hydrated adhesive layers. All figures shown are data acquired using the ZTE imaging sequence. Additional imaging was acquired on dry samples to confirm observed MR signal was from absorbed water. At least 3 of every other sample type were imaged, with representative images shown in the manuscript.

To image the water distribution changes over time, a similar ZTE sequence with 16 averages per scan was used and repeated every 10 min. The signal was integrated from a central slice through the sample in three regions: the wood core, the bond layer, and 1 mm around the edge of the wood layers.

3. Results and Discussion

Figure 1 below shows the bright signal from bound water at the adhesive bondlines.

In the image, we observe that the water signal associated with the adhesive or the water-soluble components of the PAE/Soy adhesive penetrates deeply into the wood, approximately 1 mm, and can be seen as the two bright regions of the 3-ply plywood sample. This is consistent with our previous findings reported for the Soy/PAE adhesive, where we discuss the penetration of the adhesive or water-soluble components of the adhesive penetrating into the wood to create a diffusion interphase [11]. We can say that the water is tightly bound to the soy adhesive components, resulting in the bright bondline signal. The wood also contains water because the samples were soaked and fully saturated, but the water within the wood structure is more mobile and, under the conditions of the experiment, is not seen due to the T_1 weighting of the experiment. That is, the experiment was designed to observe bound water. In this image, we also observe the grain pattern of the top and bottom layers, which are parallel to each other, and the difference in the image for the middle veneer.

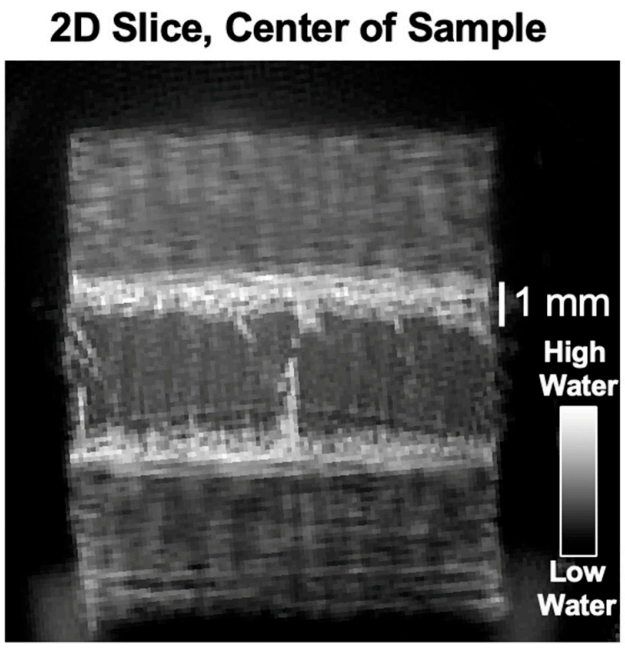

Figure 1. A two-dimensional (2D) cross-sectional image of a 3-ply plywood sample made with PAE crosslinked adhesive (Sample 67-3). The bondlines are bright in color. The sample was soaked in water for 24 h prior to imaging. Acquired using the ZTE imaging sequence. The two bond layers are visible due to the much higher signal intensities from these regions.

Figure 2 is an image of a plywood sample made with the neat soy adhesive not containing any PAE crosslinker (Sample 67-4). This sample was imaged using the same conditions as used to image Figure 1.

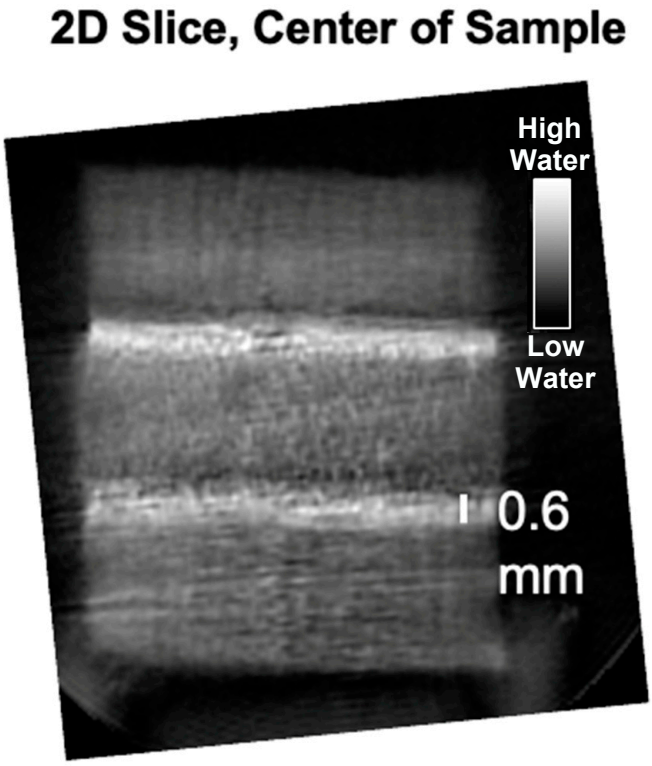

Figure 2. A two-dimensional (2D) cross-sectional image of a plywood sample made with neat soy adhesive (no PAE crosslinker) (Sample 67-4). The sample was soaked in water for 24 h prior to imaging. A central slice of the 3D ZTE image is shown.

In Figure 2, we observe that the thickness of the adhesive bondline appears smaller than that of the Soy/PAE adhesive bondline seen in Figure 1. Since the signals we observe at the bondline are associated with bound water, the difference we are seeing may be associated with the hydrophilicity of the adhesives. We have shown that PAE is very hygroscopic and plasticizes the soy adhesive [11,12]. It is possible that the presence of PAE allows for deeper penetration of the soy adhesive components, due to its greater hydrophilicity and greater mobility of the soy adhesive due to PAE as compared to the neat adhesive that does not contain PAE.

The image in Figure 2 also shows a difference in the direction of penetration of the soy adhesive. The adhesive appears to preferentially exhibit signal on the surface of the veneer where the adhesive was applied. In Figure 1, the adhesive signal seems to go into both veneers in contact with the adhesive. In Figure 2, the neat soy adhesive without PAE does not appear to penetrate the veneer above the adhesive. This can be observed as a dark line above the bright signal. We speculated that, again, this may be due to the difference in hydrophilicity and mechanical properties of the two adhesives. We also considered the possibility that the neat soy adhesive is starting to delaminate. If delamination is occurring, the water at the delaminated surface would be mobile water and not seen under the conditions used in the experiment. After the experiment was complete, the second explanation proved to be correct: the sample had delaminated, with the top veneer being more delaminated than the bottom veneer, but both bondlines had some degree of delamination.

Another experiment was conducted in which we took sample 67-3 (plywood made with Soy/PAE adhesive), removed it from the water, and sealed the sample in a glass vial. The sample was then imaged over an eight-hour period to see if we could observe any change in the intensity of the MRI signal from the sample. The data can be seen in Figure 3 below.

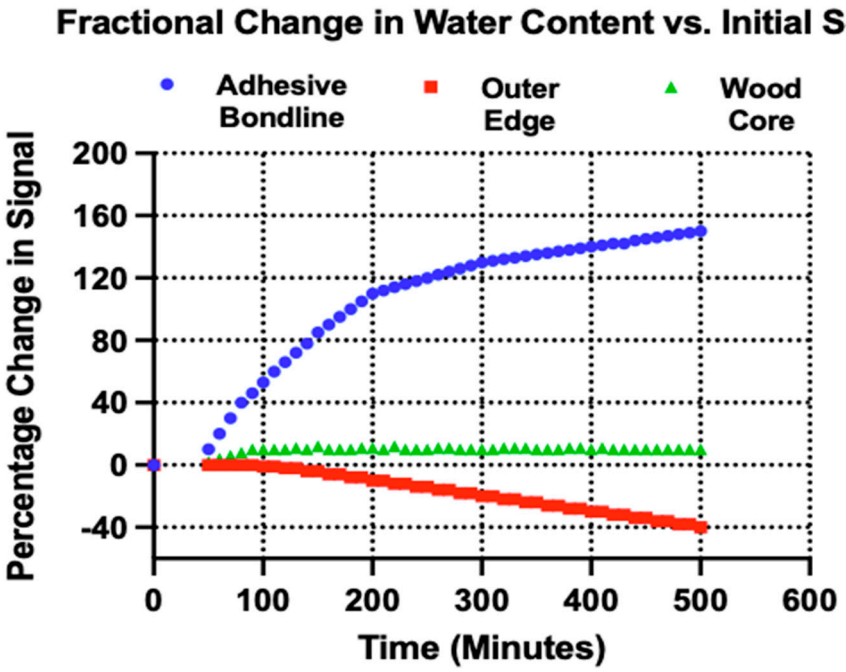

Figure 3. A plot of the change in MRI signal intensity of the plywood sample out of water as a function of time, compared to the initial signal intensity of the image in water. Three regions of interest were identified, and the signal was integrated across each region. The adhesive bondline was identified by the high signal intensity regions between wood layers, a 1 mm thick region at the outer edge of the wood layers, and the remaining regions identified as the wood core.

In this experiment, the signal intensity was measured every ten minutes as the sample sat out of water in a sealed tube. Signals were measured at the outer edge of the plywood sample, in the center of the plywood veneer, and at the soy adhesive interface. From the graph, we observe that the MRI signal at the outer edge of the plywood sample decreases slightly as a function of time. The MRI signal from the plywood veneer center (core) does not change over time. The MRI signal for the Soy/PAE adhesive bondline increases greatly over time. This experiment may indicate that moisture is migrating and concentrating at the Soy/PAE adhesive bondline. Another possible explanation is that the signal from the bound water in the soy adhesive bondline is changing due to differences in the mobility of the bound water. Either way, the data suggests that water is preferentially associated with the soy adhesive when the sample is removed from the water.

In a follow-up series of experiments, we made plywood with soy adhesive cross-linked with magnesium oxide. Two of the plywood adhesives in this experiment had some of the 200/70 soy flour substituted with surface-treated soy meal (STSM). Sample 346-2 was a plywood sample made with a neat Soy/MgO adhesive that did not contain any STSM. Sample 364-3 was a plywood sample made with a soy adhesive that had 1% of the 200/70 soy flour substituted with 1% STSM. Sample 364-4 was a plywood sample that had 2% of the 200/70 soy flour substituted with 2% STSM. The reason that the adhesive composition was made with the MgO crosslinker is that previous studies in our laboratory showed that the STSM's performed better with the MgO crosslinker as compared to the PAE crosslinker.

In addition, a plywood sample was made using a moisture-cured polyurethane adhesive (MCPU) known to impart strong, water-resistant bonds between wood veneers. This sample was labeled 346-1. The MRI below is for this MCPU plywood sample (346-1), which had been soaked in water for 24 h.

The image in Figure 4 is much different than the 2D slice images seen in Figures 1 and 2. Instead of a bright bondline associated with bound water, the bondline in this image is dark. The darkness of the bondlines is because the MCPU adhesive is impermeable to water and moisture-resistant. As such, no signal from bound water can be seen in the adhesive layer. This sample was made as a control to help define the amount of moisture resistance in the following images that contained STSM.

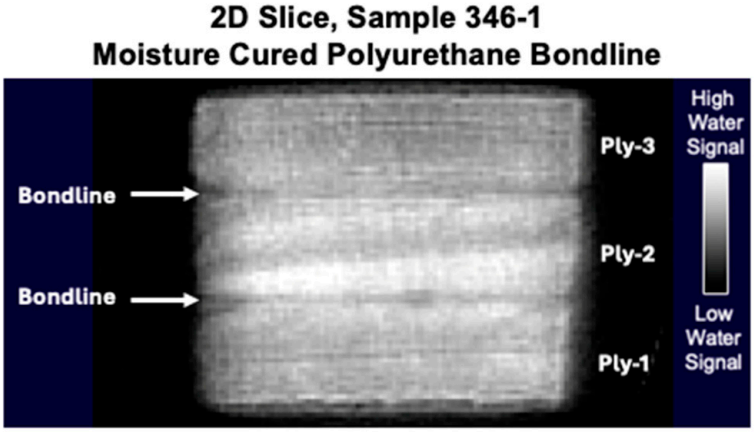

Figure 4. A two-dimensional (2D) cross-sectional image of a plywood sample made with moisture-cured polyurethane adhesive which was soaked in water for 24 h prior to imaging. A central slice of the 3D ZTE image is acquired.

Figure 5 below compares plywood samples soaked in water for 24 h. The Soy/MGO control sample (346-2) has bright, homogeneous bondlines due to appreciable signal coming from bound water associated with the soy adhesive. This is similar to what was observed

for the PAE crosslinked soy adhesive seen in Figure 1. The sample containing 1% STSM substituted for 1% of the 200/70 Soy flour used in the adhesive mixture (346-3) has much less signal at the bondlines as compared to the control. We do observe some signal from bound water within the bondline, but it is not homogeneous and is much diminished compared to the MgO control. In the sample containing 2% STSM substituted for the 200/70 soy flour in the adhesive mixture (346-4), we observe signal from the edge of the bondline but very little signal at the center of the bondline, which is dark.

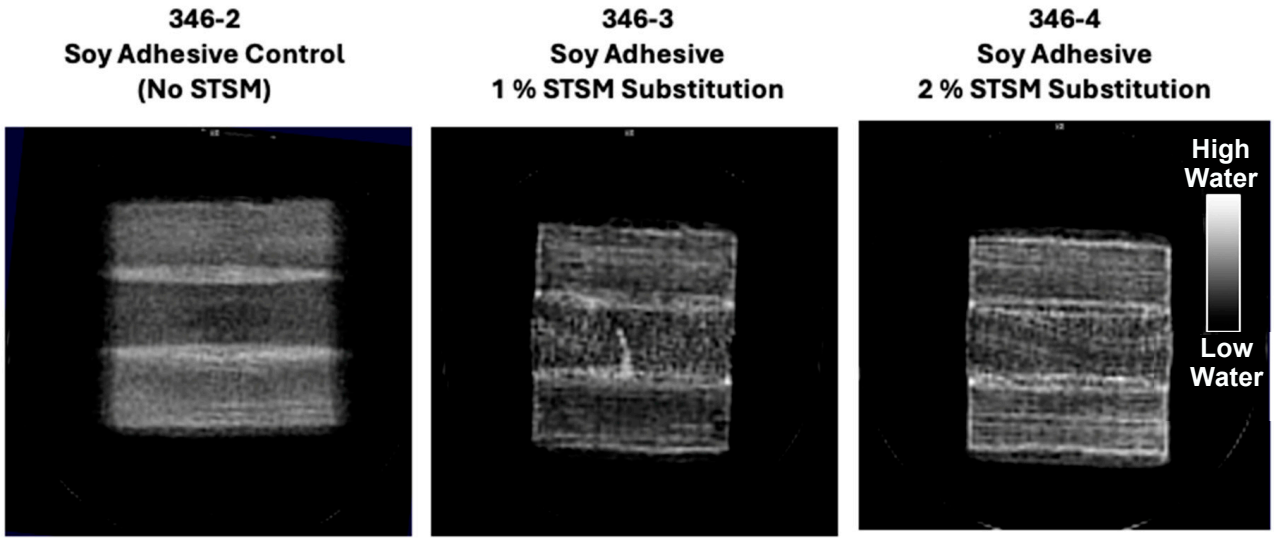

Figure 5. Two-dimensional (2D) cross-sectional images of plywood samples made with Soy/MgO adhesives containing surface-treated soy meal. The samples were soaked in water for 24 h prior to imaging. Images are scaled to the same signal intensities. The grain pattern was non-aligned in sample 346-2. These are central slices of the 3D ZTE sequence.

The zero echo time (ZET) images were reprocessed, and the data were presented in three-dimensional (3D) format. In these images, the red color indicates high water signal within the sample. Figure 6 shows the 3D images of sample 346-2, the Soy/MgO control, from two different perspectives.

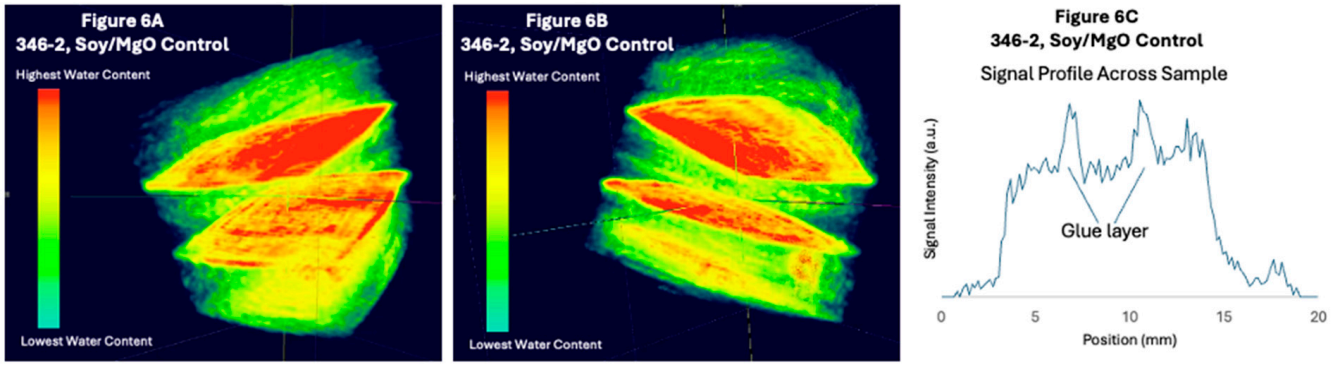

Figure 6. Three-dimensional (3D) images and Signal Intensity Profile for plywood sample 346-2 made with the Soy/MgO control adhesive that did not contain STSM. Signal intensity in arbitrary units. 3D projections of the ZTE images are shown, color-scaled to make visualization easier.

From the images in Figure 6, we can observe that the two bondlines of the plywood sample have a high signal from the bound water at the bondlines. (Figure 6A,B are two different positions of the same sample.) We can measure the water signal intensity across

the sample and plot the signal intensity in arbitrary units (au) versus position across the sample to show in graphic form that the signal is highest at the bondlines (Figure 6C).

Using the same rendering technique as shown in Figure 6, we can compare the plywood samples made with adhesives containing 1% and 2% STSM substituted for the 200/70 soy flour. These data can be seen in Figures 7 and 8.

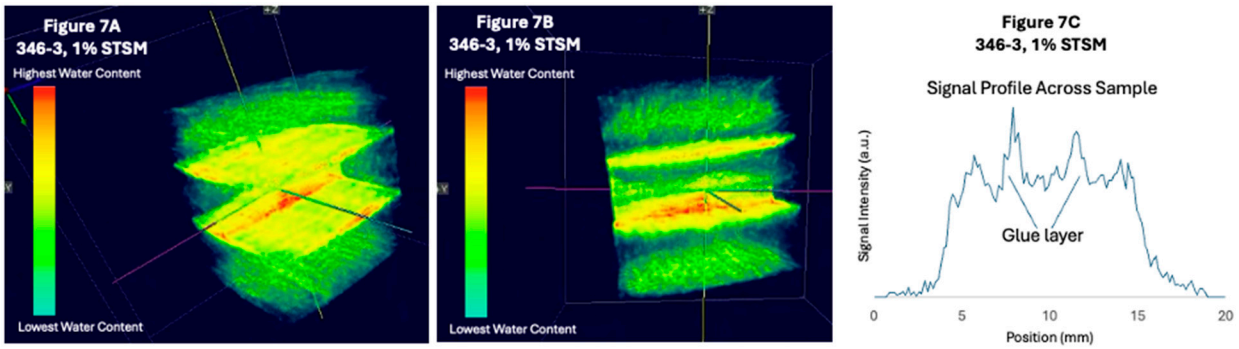

Figure 7. Three-dimensional (3D) images and Signal Intensity Profile across the sample for plywood sample 346-3 made with the Soy/MgO adhesive that contained 1% STSM. Signal intensity in arbitrary units. 3D projections of the ZTE images are shown, color-scaled to make visualization easier.

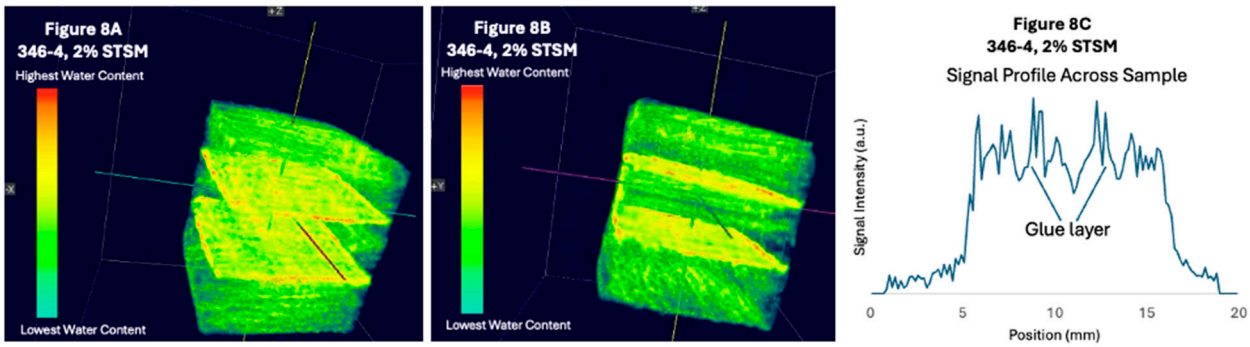

Figure 8. Three-dimensional (3D) images and Signal Intensity Profile across the sample for plywood sample 346-4 made with the Soy/MgO adhesive that contained 2% STSM. Signal intensity is in arbitrary units. 3D projections of the ZTE images are shown, color-scaled to make visualization easier.

Figure 7 shows that the incorporation of 1% STSM dramatically reduces the amount of water at the soy-adhesive bondline of this plywood sample as compared to the control sample seen in Figure 6. The signal is further diminished in Sample 346-4 Figure 8, where the Soy/MgO adhesive had 2% STSM substituted for 2% of the soy flour in the adhesive.

The plywood samples from which imaging samples 346-2, -3, and -4 were obtained were tested using ANSI/HPVA EF 2020 Section 4.2, three-cycle soak test to determine bond durability. The ANSI/HPVA 2020 test is a standardized method developed by the American National Standards Institute (ANSI) in collaboration with the Hardwood Plywood & Veneer Association (HPVA) to evaluate the performance of hardwood plywood and veneer products. This test is conducted by cutting six samples with dimensions of 127 mm by 50.8 mm (5 inches by 2 inches) from each plywood sample. The samples are then submerged in 24 °C (75 °F) water for 4 h and then dried at a temperature between 49 and 52 °C (120 and 125 °F) for 19 h. Specimens are evaluated for delamination after each cycle. Delamination is defined as separation of two plies that is greater than 50.8 mm (2 inches) in continuous length, over 6.4 mm (0.25 inches) deep at any point, and 0.08 mm (0.003 inches) wide. Ninety-five percent of specimens must pass the first cycle, and 85% must pass the third cycle. This test primarily assesses the adhesive bond quality and the moisture resistance of the bond. The data below summarizes the performance of the

plywood samples bonded with soy adhesives containing 1% and 2% STSM substituted for soy flour in the adhesive compared to the Soy/MgO control.

The data in Figure 9 shows that the Soy/MgO Control sample (346-2) exhibited strong initial bond performance, maintaining 100% bond integrity through the third cycle. However, bond strength declined in the fourth cycle, and the sample failed by the fifth cycle. In contrast, Sample 346-3, containing 1% STSM substituted for 1% Soy Flour in the adhesive formulation, performed much better. A decrease in the percentage of samples passing was not observed until the seventh cycle, and failure occurred in the ninth cycle. Sample 346-4, containing 2% STSM substituted for 2% of the Soy Flour used in the adhesive, remained at 100% passing through ten soak/dry cycles. This data is consistent with the imaging data shown in Figures 6–8. The lack of water ingress into the bondline seen in Figures 7 and 8 seems to correlate with bondline durability and moisture resistance of the soy adhesive when exposed to water.

Sample	Cycle-1	Cycle-2	Cycle-3	Cycle-4	Cycle-5	Cycle-6	Cycle-7	Cycle-8	Cycle-9	Cycle-10
346-2, Soy/MgO Adhesive Control	100	100	100	86	33					
346-3, 1 % STSM Substitution in Soy/MgO Adhesive	100	100	100	100	100	100	86	64	50	
346-4, 2 % STSM Substitution in Soy/MgO Adhesive	100	100	100	100	100	100	100	100	100	100

Figure 9. Three-cycle soak data of plywood samples 346-2, -3, and -4 obtained from ANSI/HPVA 2020 testing. The numbers represent the percentage of plywood samples that pass the soak/dry cyclic test. Green represents a pass, yellow represents a marginal result, and red represents a failure.

One hypothesis is that the substitution of the STSM is providing greater hydrophobicity to the bulk adhesive bondline and creating a tortuous path, making it harder for water to interact with the water-soluble components of the soy adhesive. As we have previously reported, water-soluble components within the soy adhesive become susceptible to moisture ingress and to dissolution, leading to the formation of a weak boundary layer [11]. The water-soluble components have been previously reported to consist of a variety of polypeptides and carbohydrates [11,18]. These water-soluble components undergo partitioning during hot-pressing of the plywood and become concentrated at the adhesive-wood interface. This weak boundary layer leads to stress concentrations at the wood/adhesive interface, and delamination occurs. It is possible that the tortuous path created by the hydrophobic STSM slows the water ingress and slows the dissolution of these components.

4. Conclusions

Using MRI to study moisture ingress at an adhesive bondline offers the ability to non-destructively visualize where the moisture is and to qualitatively discern the areas of the sample that have greater concentrations of bound water. In addition, it may be possible with future experiments not only to visualize the water at the bondline, but to also calculate diffusion kinetics of moisture into or out of the bondline. It is further possible that this form of non-destructive testing can be correlated to bond strength and moisture resistance of the bondline.

MRI of soy adhesive bondlines within plywood composites provides insight into moisture-induced degradation of soy adhesive bonds. The incorporation of hydrophobically treated soy meal as an additive to the soy adhesive resulted in much lower moisture

observed at the bondlines and positively contributed to the bondline durability, as observed in the three-cycle soak testing.

Author Contributions: Conceptualization, J.J.M. and A.A.P.; Methodology, J.J.M., A.A.P., J.H.P.C. and J.T.; Formal analysis, J.J.M., A.A.P. and J.H.P.C.; Investigation, J.J.M., A.A.P., J.H.P.C. and J.T.; Writing—original draft, J.J.M.; Writing—review & editing, J.J.M.; Project administration, J.J.M.; Funding acquisition, J.J.M. All authors have read and agreed to the published version of the manuscript.

Funding: The authors would like to thank the United Soybean Board for funding this research (Project #25-101-D-C-1A and Project #25-101-D-C-1B). We also acknowledge the University of Florida, McKnight Brain Institute at the National High Magnetic Field Laboratory's Advanced Magnetic Resonance Imaging and Spectroscopy (AMRIS) Facility. The facility is supported by National Science Foundation Cooperative Agreement DMR- 1644779 and the State of Florida.

Data Availability Statement: The raw data supporting the conclusions of this article will be made available by the authors on request.

Conflicts of Interest: Joseph J. Marcinko was employed by the company Polymer Synergies LLC, Anthony A. Parker was employed by the company A.A. Parker Consulting LLC, Josh Tyler was employed by the company Columbia Forest Products. The remaining authors declare that the research was conducted in the absence of any commercial or financial relationships that could be construed as a potential conflict of interest.

References

1. Ishida, H. *Characterization of Composite Materials*, 1st ed.; Materials Characterization Series; Momentum Press: Buchanan, NY, USA, 2009; p. 277.
2. Brown, R.W.; Cheng, Y.C.N.; Haacke, E.M.; Thompson, M.R.; Venkatesan, R. *Magnetic Resonance Imaging: Physical Principles and Sequence Design*, 1st ed.; John Wiley & Sons: Hoboken, NJ, USA, 2014; p. 914.
3. Callaghan, P.T. *Principles of Nuclear Magnetic Resonance Microscopy*, 1st ed.; Oxford University Press Inc.: New York, NY, USA, 1991; p. 516.
4. Nieminen, A.O.K.; Liu, J.; Koenig, J.L. NMR imaging of adhesive-bonded structures: The use of the T1 and T2 relaxation time information. *J. Adhes. Sci. Technol.* **1989**, *3*, 455–462. [CrossRef]
5. Olson, J.R.; Chang, S.J. Nuclear magnetic resonance imaging: A noninvasive analysis of moisture distributions in white oak lumber. *Can. J. For. Res.* **1990**, *20*, 586–591. [CrossRef]
6. Hall, L.D.; Rajanayagam, V.; Stewart, W.A.; Steiner, P.R. Magnetic resonance imaging of wood. *Can. J. For. Res.* **1986**, *16*, 423–426. [CrossRef]
7. Bucur, V. Nuclear magnetic resonance. In *Nondestructive Characterization and Imaging of Wood*; Springer: Berlin, Germany, 2003; pp. 215–279.
8. Stenstrom, S.; Bonazzi, C.; Foucat, L. Magnetic resonance imaging for determination of moisture profiles and drying curves. In *Modern Drying Technology: Experimental Techniques*; Tsotsas, E., Mujumdar, A.S., Eds.; Wiley-VCH Verlag GmbH & Co. KGaA: Weinheim, Germany, 2009; pp. 91–142.
9. Florance, E.R. Magnetic resonance imaging (MRI) of oak trees infected with Phytophthora ramorum to determine potential avenues of infection in bark. In *Proceedings of the Sudden Oak Death Second Science Symposium: The State of Our Knowledge, Monterey, CA, USA, 18–21 January 2005*; Lewis & Clark College: Portland, OR, USA, 2005. [CrossRef]
10. Lekoa, J.; Richmana, R.; Schumacher, C. Applicability of magnetic resonance imaging for mass timber moisture research. *Constr. Build. Mater.* **2025**, *489*. [CrossRef]
11. Marcinko, J.; Parker, A. Spectroscopic Characterization of the Chemical Changes Occurring in Soy Wood Composite Adhesives When Exposed to Moisture. *For. Prod. J.* **2024**, *74*, 143–150. [CrossRef]
12. Parker, A.; Marcinko, J. Dynamic mechanical and spectroscopic studies of soy flour adhesives. *Express Polym. Lett.* **2026**, *20*, 594–616. [CrossRef]
13. Jang, Y.; Li, K. An All-Natural Adhesive for Bonding Wood. *J. Am. Oil Chem. Soc.* **2015**, *92*, 431–438. [CrossRef]
14. *ANSI-HPVA-HP-1-2020*; Standard for Hardwood and Decorative Plywood. American National Standards Institute: New York, NY, USA, 2020. Available online: https://www.ansi.org (accessed on 15 September 2026).
15. Weiger, M.; Pruessmann, K.P. MRI with Zero Echo Time. *eMagRes* **2012**, *1*, 311–321.
16. Madio, D.P.; Lowe, I.J. Ultra-fast imaging using low flip angles and fids. *Magn. Reson. Med.* **1995**, *34*, 525–529. [CrossRef] [PubMed]

17. Haase, A.; Frahm, J.; Matthaei, D.; Hanicke, W.; Merboldt, K.-D. FLASH imaging: Rapid NMR imaging using low flip angle pulses. *J. Magn. Reson.* **1986**, *67*, 258–266. [CrossRef]
18. Frihart, C.R.; Birkeland, M.J. Soy properties and soy wood adhesives. In *Soy-Based Chemicals and Materials*; Brentin, R.P., Ed.; American Chemical Society: Washington, DC, USA, 2014; Volume 1178, pp. 167–192.

Disclaimer/Publisher's Note: The statements, opinions and data contained in all publications are solely those of the individual author(s) and contributor(s) and not of MDPI and/or the editor(s). MDPI and/or the editor(s) disclaim responsibility for any injury to people or property resulting from any ideas, methods, instructions or products referred to in the content.